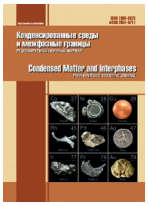

ISSN 1606-867X (Print)
ISSN 2687-0711 (Online)
Condensed Matter and Interphases
Kondensirovannye Sredy i Mezhfaznye Granitsy
https://journals.vsu.ru/kcmf/

Original articles

Research article
https://doi.org/10.17308/kcmf.2022.24/10561

Anodic oxide coatings with a hierarchical micronanostructure on sintered titanium powders

N. M. Yakovleva[1]✉, A. M. Shulga[1], I. V. Lukianchuk[2], K. V. Stepanova[1], A. N. Kokatev[1], E. S. Chubieva[1]

[1]Petrozavodsk State University,
33 Lenina prospekt, Petrozavodsk 185910, Russian Federation

[2]Institute of Chemistry of the Far Eastern Branch of the Russian Academy of Sciences,
159 100-Letiya Oktyabrya ul., Vladivistik 690022, Russian Federation

Abstract

TiO_2 nanotubes formed by electrochemical anodising of Ti (titanium foil) are normally X-ray amorphous. To improve their functional properties, they are usually converted into crystalline nanotubes by annealing at $T \approx 400–500$ °C. What is more, under certain conditions, oxide films with a hierarchical micronanostructure can be formed on titanium foil by anodising in fluorine-containing electrolytes. Such films contain nanostructured microcones whose atomic structure corresponds to anatase (α-TiO_2). It is interesting to find out whether it is possible to form anodic oxide coatings with a hierarchical micronanostructure on the surface of sintered powders of titanium sponge, which should have much larger specific surfaces and a wider range of applications. This paper is aimed at the study of the process of anodising porous samples of sintered powders of titanium sponge in an aqueous electrolyte (1 M H_2SO_4 + 0.15 wt % HF).

The object of our study were sintered titanium powders in the form of samples of porous powder materials with a specific area of S_{sp} = 1,350 cm^2/g. Anodising was conducted in a 1 M H_2SO_4 + 0.15 wt % HF electrolyte at various values of current density (j_m). Surface morphology before and after anodising was investigated by scanning electron microscopy and atomic force microscopy. X-ray diffractometry was used to study the phase composition.

The research involved the study of the influence of conditions for the galvanostatic anodising of samples of porous powder materials made from titanium sponge on the growth, morphology, and atomic structure of anodic oxide coatings. For the first time, it was shown that anodising at the values of current density j_m = (230÷1,890) mA/g leads to the appearance of nanostructured α-TiO_2 microcones (with base diameters and heights of up to 4 μm) in an amorphous nanoporous/nanotube oxide matrix (with an effective pore/tube diameter of about 50 nm). Since such coatings have a high specific area and a hierarchical micronanostructure, they are promising for the design of devices for photocatalytic environment purification and production of superhydrophobic surfaces.

Keywords: Sintered powders, Porous powder materials, Titanium sponge, Anodic oxide coatings, Structure hierarchy, Microcones, Crystalline, Nanostructured titanium dioxide, Scanning electron microscopy, Atomic force microscopy

Funding: The study was carried out within the framework of the R&D Support Programme for Undergraduate and Postgraduate Students of Petrozavodsk State University funded by the Government of the Republic of Karelia (agreement KGRK-21/H2-05 dated of 30.03.2022) and partially by the federal budget funds allocated for the implementation of the state assignment for the Institute of Chemistry of the Far Eastern Branch of the Russian Academy of Sciences (topic No. FWFN (0205) -2022-0001).

Acknowledgements: X-ray diffraction and scanning electron microscopy were performed using the equipment of the centres for collective use of the Karelian Research Centre of the Russian Academy of Sciences (Petrozavodsk) and the Institute of Chemistry of the Far Eastern Branch of the Russian Academy of Sciences (Vladivostok), respectively.

✉ Natalia M. Yakovleva, e-mail: nmyakov@gmail.com

For citation: Yakovleva N. M., Shulga A. M., Lukianchuk I. V., Stepanova K. V., Kokatev A. N., Chubieva E. S. Anodic oxide coatings with a hierarchical micronanostructure on sintered titanium powders. *Condensed Matter and Interphases.* 2022;24(4): 572–583. https://doi.org/10.17308/kcmf.2022.24/10561

Для цитирования: Яковлева Н. М., Шульга А. М., Лукиянчук И. В., Степанова К. В., Кокатев А. Н., Чубиева Е. С. Анодно-оксидные покрытия с иерархической микронаноструктурой на спеченных порошках титана. *Конденсированные среды и межфазные границы*. 2022; 24(4): 572–583. https://doi.org/10.17308/kcmf.2022.24/10561

1. Introduction

Electrochemical anodising allows forming TiO_2 films directly on titanium substrates. Depending on the process parameters such as electrolyte composition and concentration, voltage/current, and the duration of anodising, anodic oxide coatings (AOCS) of different morphologies and atomic structures can be created.

Anodising Ti in fluorine-containing electrolytes results in the formation of self-organised nanotube or nanoporous AOCs with evenly distributed nanosized structural elements (tubes or pores) [1–7]. TiO_2 nanotubes obtained by electrochemical anodising are normally X-ray amorphous. In many cases, amorphous nanotube AOCs are converted into crystalline AOCs by annealing at $T \approx 400–500$ °C to improve their functional properties (catalytic activity, electronic conductivity or mechanical strength), which expands the range of their applications [1,2,6]. Therefore, it is important to form anodic TiO_2 nanotubes with a crystalline structure without any additional thermal treatment. A number of methods for Ti anodising have been proposed. They allow obtaining TiO_2 nanotubes at room temperature with a crystalline component in the form of anatase (hereinafter, α -TiO_2) and completely crystalline α-TiO_2 nanotubes at $T = 60$ °C [3, 8, 9]. In particular, some authors have reported one-stage synthesis of arrays of α-TiO_2 crystalline nanotubes by anodising at room temperature by using polyols [10]. Despite certain technological difficulties, researchers have been actively developing the method for converting amorphous TiO_2 nanotubes into crystalline nanotubes with a α-TiO_2 structure by water or water vapour treatment [11–13].

Over the past 10 years, a number of works [14–20] have shown that under certain conditions of anodising titanium foil in fluorine-containing aqueous electrolytes, oxide coatings can be formed, whose amorphous matrix has microcone α-TiO_2 formations. Thus, in 2011, Wang C. et al. [14] reported about a method of anodising Ti foil (99.6%) in aqueous solutions of NH_4F at room temperature which resulted in the formation of AOCs, on the surface of which there were homogeneously distributed cone-shaped micron formations with a α-TiO_2 structure. According to the authors, the shape of crystalline formations was flower-like, although it would be more appropriate to call them "microcones" given their geometric shape and dimensional parameters. Each microcone, in its turn, was nanostructured and had a set of layers with a thickness of about 20 nm. It should be noted that similar α-TiO_2 structures were also found when studying the formation of AOCs on titanium foil in aqueous solutions of acids (sulphuric, orthophosphoric) without adding fluorine [21–25].

Later, it was reported that similar oxide films on Ti were obtained in aqueous solutions of acids (H_3PO_4, H_2SO_4, and $C_2H_2O_4$) with a HF additive [17–20]. It was found that the critical parameters affecting the appearance of α-TiO_2 microcones in the amorphous oxide matrix are the value of the applied potential and the concentration of the fluorine-containing additive (NH_4F [14–16] or HF [17–20]). Due to their high surface area, morphological regularity, and a crystalline structure, α-TiO_2 micronanostructures obtained at room temperature directly on a titanium substrate can be used in various ways. For example, they are a promising material for water photoelectrolysis, solar energy conversion [14], and the manufacture of lithium-ion battery anodes [20, 26, 27]. At present, only the initial assumptions have been made about the mechanism of the formation of anatase microcones when anodising titanium foil in aqueous solutions with fluorine ions. Therefore, this issue needs to be further researched.

Porous powder materials (PPM) obtained by pressure treatment and the sintering of Ti sponge powders are characterised by a set of unique physicochemical properties, including antibacterial effect, accelerated osseointegration with bone tissues, etc. [28, 29]. The formation of nanostructured AOCs on the surface of sintered

powder particles should lead to a noticeable increase in the specific area of the sample and a range of its functional applications. In [7], it was shown for the first time that under certain conditions of anodising samples of titanium sponge PPM samples (hereinafter, TS PPM) in a 1 M H_2SO_4 + 0.15 wt% HF aqueous electrolyte, an X-ray amorphous TiO_2 film with a thickness of about 300 nm was formed on the surface of the sintered powder microparticles. This film was characterised by the presence of evenly distributed open pores/tubes with effective diameters between 30 and 70 nm. What is more, the microinhomogeneous surface of anodised samples both had areas with pores and areas with tubular structures. There is no information on the formation of anodic oxide coatings (AOCS) with hierarchical micronanostructures on the surface of sintered powders of sponge titanium, that is why it is very important to find out whether it is possible to obtain coatings of this type. For this purpose, this paper studies the process of anodising porous materials made from sintered powders of Ti sponge in a 1 M H_2SO_4 + 0.15 wt % HF aqueous electrolyte.

2. Experimental

In our study, we used sintered titanium powders in the form of samples of porous powder materials (PPM). PPM samples were prepared by pressing sponge powder of technically pure titanium with a fraction of 0.63-1.0 mm at 100–120 MPa followed by vacuum sintering at a temperature of 1,090°C for 70 minutes. As a result, we obtained disc-like samples with a diameter of 20–30 mm, a thickness of 3 mm, and a specific area of S_{sp} = 1,350 cm^2/g [7,28,30].

The samples were preliminarily degreased in acetone and ethanol in an ultrasonic bath, washed in distilled water, and dried in the air. Anodising was performed in three-electrode electrochemical cells with a tantalum cathode and platinum counter electrode in a 1 M H_2SO_4 + 0.15 wt% HF aqueous electrolyte at room temperature in a galvanostatic mode (GSM). To determine the cell current during galvanostatic anodising of sintered powders, it is necessary to know the surface area of the sample, which can be found if the value of the specific surface, S_{sp}, is known. Thus, to anodise TS PPMs with a mass of m = 1 g and S_{sp} = 1,350 cm^2/g at a current density j_a = 0.15 mA/cm^2, it is necessary to set the value of the cell current at $I_a \approx 202$ mA. When anodising samples of sintered powders of various sizes (masses) under galvanostatic conditions, it is advisable to compare voltage-time transients in the electrolytic cell, $U_a(t)$, obtained at constant current values per unit mass of the sample $j_m = I_a/m$ (mA/g) [31].

In this work, anodising was carried out at the values of j_m = 202, 230, 405, and 1,890 mA/g. Normally, the duration of the process was t_a = 1 hour. At j_m = 1,890 mA/g, we studied anodising for t_a = 45, 60, and 90 min. During the growth of AOCs, voltage-time transients, $U_a(t)$, were recorded using an ERBIY-7115 electronic recorder connected to a computer. The detailed description of the anodising method is presented in the works [7, 31–33].

Scanning electron microscopy (SEM), atomic force microscopy (AFM), and X-ray diffraction were used to study the morphology, elemental composition, and atomic structure of the samples. The surface morphology of the samples before and after anodising was investigated by SEM using high-resolution microscopes *Mira* (*Tescan*, Czech Republic) and S-55009 (*Hitachi*, Japan). The elemental composition was evaluated by energy dispersive X-ray spectroscopy (EDS) using a *Thermo Scientific* attachment (USA). The data were collected for 5–10 sections, including those of microscopic size (up to 50×50 μm^2) as well as "dots" of 50×50 nm^2 and 10×10 nm^2. The sections were chosen according to previously obtained SEM images of the surface and their elemental composition was quantitatively analysed.

The AFM studies were conducted in air on a Solver Next (ZAO NT-MDT, Russia) scanning probe microscope in a tapping mode. High-resolution diamond-like carbon tips (*NSG*01) with the length of 125 μm, resonance frequency of 87-230 kHz, and curvature radius of the needle of 10 nm were used. The size of the scan area varied in the range from 1 to 25 μm^2. From 2 to 5 surface sections were scanned. The thickness of the oxide films was assessed by AFM images of the samples [7]. The sequence of processing AFM images is described in [32].

X-ray diffractometry was used to study the phase composition. The samples were studied

using the X-ray technique before and after anodising on a *D8 ADVANCE* (Bruker, Germany) automated diffractometer using CuK_α radiation in the angular range 2θ = (10–90)° at 0.02° intervals. The phase composition of AOCs was identified by comparing a set of d-spacings calculated according to the experimental data and the corresponding values for Ti and crystalline modifications of titanium oxides.

3. Results and discussion

The first stage of the research of galvanostatic anodising of porous samples of sintered powders of Ti sponge in a 1 M H_2SO_4 + 0.15 wt% HF aqueous electrolyte involved the study of the growth kinetics of anodic oxide coatings (AOCs) at constant current values per unit mass of the sample, j_m, equal to j_m = 202, 230, 405, and 1,890 mA / g. Figure 1 shows the voltage-time transients in the electrolytic cell, U_a(t), registered during the growth of AOCs. We can see that $U_a(t)$ changed noticeably with an increase in the current value.

At values of j_m = 202 and 230 mA/g, during the first 30 minutes of the process, kinetic dependencies (Fig. 1, curves *1* and *2*) corresponded well to the growth of self-organised porous/tubular AOCs [2, 7, 32] and were characterised by the values of steady-stage voltage between 5 and 9 V. There were successively distinguished sections of $U_a(t)$ curves that are commonly interpreted as those corresponding to different stages of the formation of self-organised oxide films: the growth of a barrier layer, initiation and self-organisation of pores, and the steady-state growth of the porous/tubular layer. However, further voltage began to grow and reached values of about 20 V (j_m = 202 mA/g) and 30 V (j_m = 230 mA/g) at the end of the process (t_a = 1 h).

The dependencies $U_a(t)$ (Fig. 1, curves *3*-*6*) recorded at large current values, j_m = 405 mA/g and j_m = 1,890 mA/g, were also close to the typical galvanostatic growth curves of self-organised porous/tubular AOCs. However, the value of steady-stage voltage in such conditions was noticeably higher and close to U_a^{st} ~ (25–27) V. Also, at j_m = 405 mA/g (Fig. 1, curve *3*), 60 minutes of anodising was required for the transition to the stage of steady-state growth, while at j_m = 1,890 mA/g, it took 40 minutes (Fig. 1, curves *4*–*6*). We can see that at j_m = 1,890 mA/g, the variation of the anodising time between 45 and 90 minutes practically did not cause any changes in $U_a(t)$. It should be noted that the presence of numerous voltage peaks at the stage of self-organisation and the steady-state growth of pores was characteristic of $U_a(t)$ obtained both at j_m = 405 mA/g and j_m = 1,890 mA/g (Fig. 1, curves *3* and 4). Such voltage behaviour can be caused by multiple local breakdowns in the barrier layer [35]. The analysis of the initial sections of the $U_a(t)$ transients for all of the used values of j_m, with the exception of j_m = 202 mA/g, showed [31] that in the initial sections, a few seconds after the beginning of anodising, there was a change in the slope of $U_a(t)$, which is usually associated with the appearance of the crystalline component α-TiO_2 in the composition of the amorphous oxide layer [34].

During the next stage, a microscopic study of the surface morphology of the samples before and after anodising was conducted using SEM. According to the data [7], the surface relief of the sample before anodising indicated a sufficiently developed structure characteristic of a titanium sponge [28, 36]. The analysis of the elemental composition of the samples before anodising showed that its main element was Ti (C_{Ti} ≈ 90–100 wt%). The presence of C (between 5.5 and 9 wt%) was also established. It was found that some areas had individual defects (micron inclusions whose composition included Si, Ca, Al,

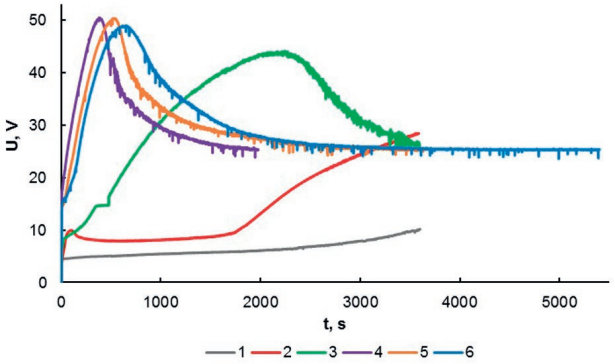

Fig. 1. Voltage-time transients, $U_a(t)$, recorded during anodising of the samples of porous powder materials made from titanium sponge in a 1 M H_2SO_4 + 0.15 wt % HF solution at different values of current j_m: 202 mA/g (curve *1*, t_a = 60 min); 230 mA/g (curve *2*, t_a = 60 min); 405 mA/g (curve *3*, t_a = 60 min); 1,890 mA/g (curves *4*–*6*, t_a = 45, 60, 90 min)

and O (up to 20 wt%), which corresponds to the state standard GOST 17746-96 Titanium sponge.

Fig. 2 shows that after anodising at j_m = 202 mA/g, the surfaces of the TS PPM samples had self-organised AOCs with open pores and effective diameters from 40 to 60 nm, which corresponds well to the results [7]. The estimation based on the pore size and the thickness of the oxide layer [7] showed that the surface area of TS PPM samples anodised under such conditions would increase by approximately 10 times.

The study of the morphology of AOCs anodised at j_m = 230 mA/g (t_a = 1 h) mainly revealed regions with a regular-porous relief similar to that shown in Fig. 2. It also revealed separate regions containing a set of rounded formations with a size of 0.2 to 2.0 μm (Fig. 3 a,b) which, according to the results [3,34,35], can be interpreted as crystalline nuclei with a α-TiO_2 structure (anatase).

After anodising at j_m = 405 mA/g, unevenly distributed rounded formations of cone-like morphology were observed on the surface of all studied areas of the porous oxide layer (Fig. 4). Their shape was close to conical, their estimated base diameters were between 0.7 and 3.5 μm and their heights were between 0.3 and 3.0 μm (Fig. 4 b, c), which allows calling them microcones (MCC). Each formation, in its turn, was a set of heterogeneous layers with a thickness of about 20–35 nm (Fig. 4c), i.e. they were nanostructured. There were cracks around the cone-like MCCs and separate depressions, craters (Fig. 4b). It can be assumed that the craters had been filled with MCCs. It means that after anodising for t_a = 60 min at j_m = 230 mA/g, multilayer formations only began to appear on the surface of the porous/tubular oxide film, while at j_m = 405 mA/g, their number and size increased.

During the final stage, we examined the surface of AOCs obtained at j_m = 1,890 mA/g. Despite bubbling the electrolyte, by the end of the anodising process the temperature near the surface of the sample increased by 15-20°C. Anodising at j_m = 1,890 mA/g for 45 minutes (Fig. 5a) resulted in the uneven distribution of multilayer conical formations of various sizes on the surface of the samples with porous/tubular AOCs. The values of their base diameters varied between 0.8 and 3.0 microns, and their heights varied between 0.8 and 4.0 microns. The thickness of the layers was about 30 nm. As compared to the MCCs formed by anodising at j_m = 405 mA/g (Fig. 4), these MCCs were more elongated and their height in most cases exceeded their base diameter. The analysis of SEM images obtained at larger magnification suggests that the MCC layers were nanoporous, which is consistent with the data in [26]. All studied areas within most MCCs were characterised by cracks around the bases with a width of ~90–150 nm. Cracks also appeared in the areas between MCCs, the number of craters with diameters between 1.0 and 2.5 μm

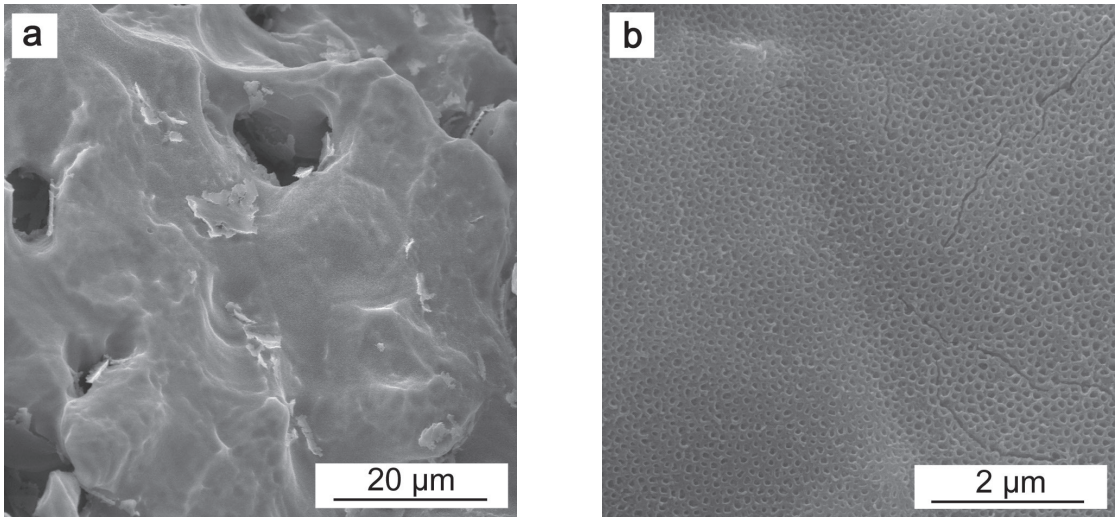

Fig. 2. SEM images of the surface of the samples of porous powder materials made from titanium sponge after anodising in a 1 M H_2SO_4 + 0.15 wt % HF electrolyte for 1 hour at $j_m \cong$ 202 mA/g. The images were obtained at various magnifications (a, b)

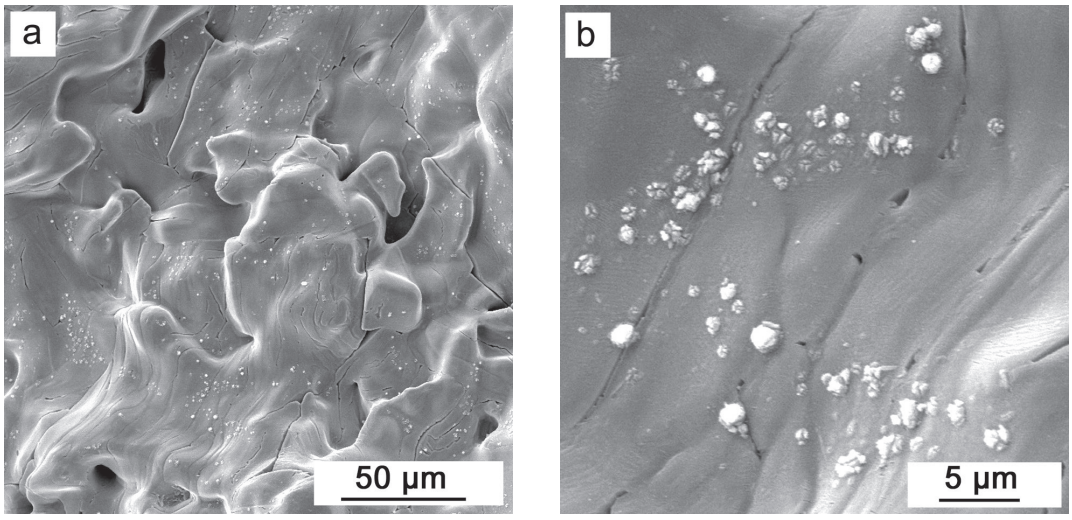

Fig. 3. SEM images of sections on the surface of the samples of porous powder materials made from titanium sponge after anodising in a 1 M H_2SO_4 + 0.15 wt % HF electrolyte for 1 hour at $j_m \cong 230$ mA/g. The images were obtained at various magnifications (a, b)

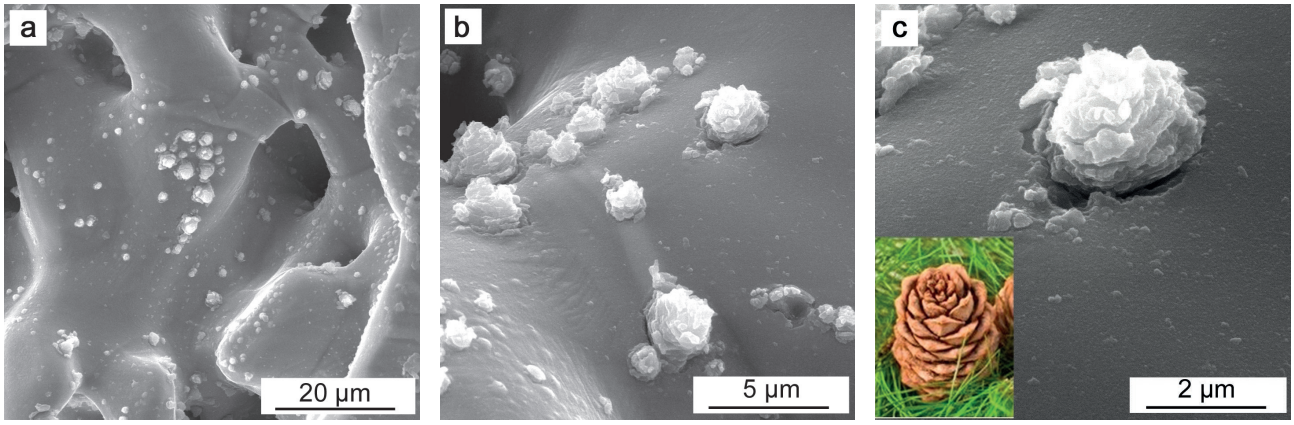

Fig. 4. SEM images of a section on the surface of the samples of porous powder materials made from titanium sponge after anodising in a 1 M H_2SO_4 + 0.15 wt % HF electrolyte for 1 hour at $j_m \cong 405$ mA/g. The images were obtained at various magnifications (a, b, c)

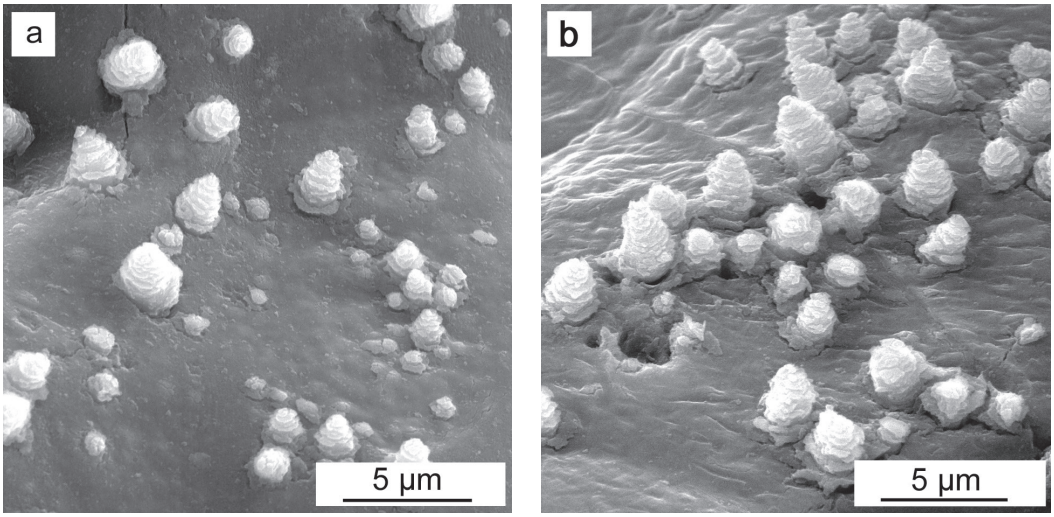

Fig. 5. SEM images of the surface of the samples of porous powder materials made from titanium sponge after anodising in a 1 M H_2SO_4 + 0.15 wt % HF electrolyte for 45 (a) and 60 (b) min at $j_m \cong 1{,}890$ mA/g

also increased. Increasing the anodising time to t_a = 60 min did not result in any noticeable changes in the appearance of the AOC surface. Multilayer MCCs were unevenly distributed on the surface of the AOCs, the diameters of their bases were in the range from 0.8 to 3.0 μm, their heights were between 1.9 and 4.1 μm (Fig. 5b), and the number of craters and cracks between microcone formations increased. The AFM was used to study in detail the surface relief of the AOC sections between large microcone formations. It can be seen (Fig. 6a, b) that along with surface areas characterised by the presence of regular open pores/tubes (d_p ~ 20–30 nm), there were unevenly distributed cone-shaped formations with base diameters in the range from 50 to 200 nm and heights below 200 nm. This means that anodising at a current value of j_m = 1,890 mA/g for t_a = 60 min leads to the formation of nanoporous/nanotubular oxide coatings on microparticles of porous powder samples. These coatings have multilayer conical formations whose base diameters and heights vary over a wide range.

After t_a = 90 min, the studied sections of the AOC surface had multilayer MCCs with base diameters between 0.6 and 3.9 μm and heights between 1.7 and 4.5 μm. The number of craters sharply increased and their estimated diameters were between 0.3 and 3.0 μm (Fig. 7). The elemental composition of AOCs which were formed within t_a = 90 min was studied within different areas: (I) within microcones, (II) between craters/microcones, (III) in the conjugation area of craters and the surface of the AOC, (IV) at the bottom of craters (Table 1). The obtained data indicate that the MCCs had Ti and O in their composition. The values of weight percent of the elements were $C_{Ti} \approx 60$ wt %, $C_O \approx 40$ wt%, which corresponded well to TiO_2. Additionally, an insignificant amount of F (up to 4 wt%) was found in some microcones. The elemental composition of AOCs outside cones and craters also corresponded to TiO_2. There were traces of sulphur S (less than 0.2 wt%). The presence of S could be due to the inclusion of SO_4^{2-} anions into the porous oxide layer of AOCs during its growth [36]. All studied surface sections were characterised by the presence of 2 to 10 wt% of carbon. It was found that only titanium was present at the bottom of the craters.

Next, an X-ray technique was used to examine the phase composition of the samples before and after anodising at j_m = 1,890 mA/g for 60 and 90 min. In addition to reflections from the titanium substrate, the XRD patterns of the studied samples after anodising had several additional low-intensity lines. Fig. 8 shows a typical XRD pattern of a sample anodised in 1 M H_2SO_4 + 0.15 wt % HF solution at a current value of j_m = 1,890 mA/g for t_a = 90 min. Identification of the diffraction lines on the XRD patterns of powder samples is a very challenging task, firstly, due to their low intensity and, secondly, due to the coincident positions of several Bragg reflections. Hence the need for repeated X-ray examination of the samples and strict compliance with the accuracy requirements when aligning the studied object. As a result, we identified isolated

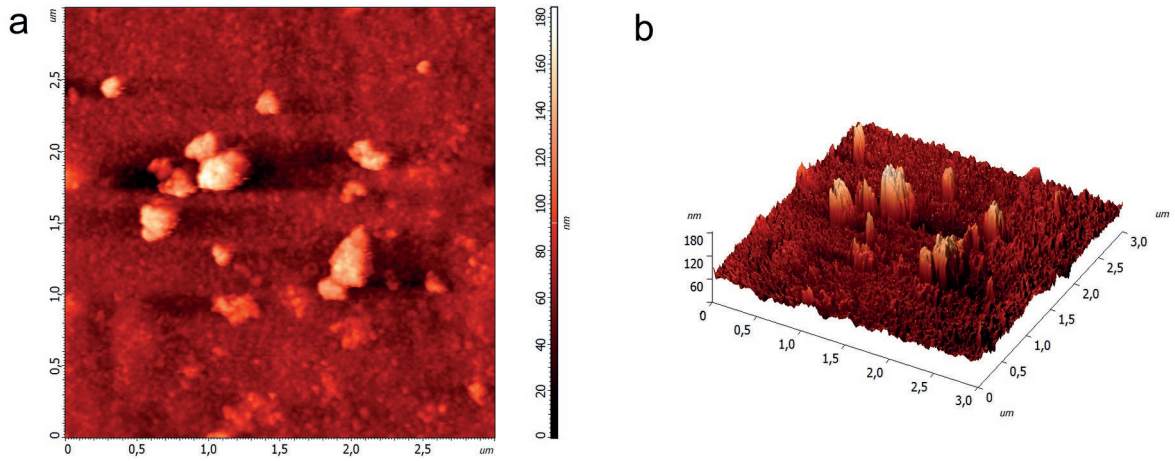

Fig. 6. AFM images (2D - a, 3D - b) of the surface of the samples of porous powder material made from titanium sponge after anodising in a 1 M H_2SO_4 + 0.15 wt % HF electrolyte for 1 hour at $j_m \cong$ 1,890 mA/g.

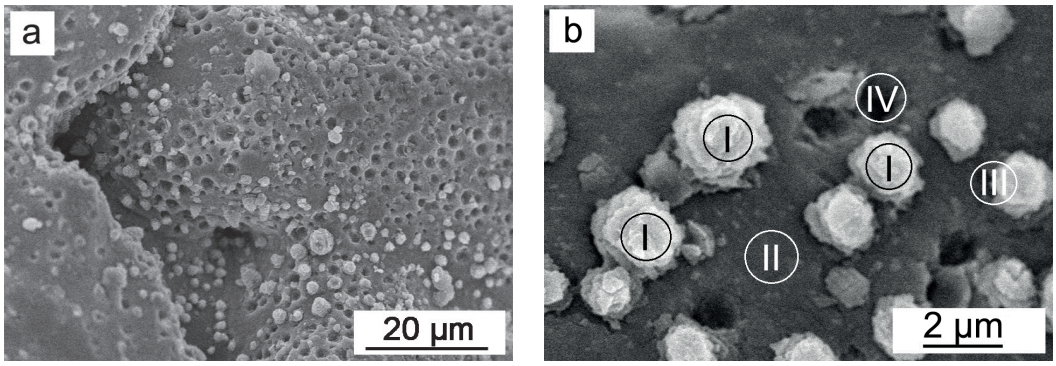

Fig. 7. SEM images of a section on the surface of the sample of porous powder material made from titanium sponge after anodising in a 1 M H_2SO_4 + 0.15 wt % HF electrolyte for 90 min at $j_m \cong 1{,}890$ mA/g. The images were obtained at various magnifications (a, b) The results of the EDX analysis of the elemental composition of sections I–IV (b) are presented in Table 1

Table 1. The main elemental composition of sections I-IV (Fig. 7B) on the surface of the samples of porous powder materials made from titanium sponge after anodising in a 1 M H_2SO_4 + 0.15 wt% HF electrolyte for 90 min at j_m 1,890 mA/g

Element	Mass fraction of the element, C, wt%			
	I	II	III	IV
C	10.0±1.9	5.3±1.3	6.9±1.8	–
O	35.2±3.2	41.4±2.9	33.5±3.3	–
Ti	54.8±1.8	53.2±0.3	59.6±3.5	100.0±1.8

lines corresponding to the Bragg reflections (101) and (200) for α-TiO_2 with d-spacings: d_1 = 0.351 nm (101), d_2 = 0.189 nm (200). In addition, the asymmetry of the line (002) Ti (d = 0.234 nm) may indicate [17] the presence of a reflection corresponding to the reflection (004) for α-TiO_2 with d_3 = 0.239 nm. This fact suggests that the phase composition of the microcone formations included in the X-ray amorphous nanoporous/nanotubular titanium oxide matrix corresponded to the crystalline modification of TiO_2 (anatase). It should also be emphasised that the results of qualitative phase analysis correlate with the data in papers [16-18] devoted to a comprehensive study of the atomic structure of microcone formations in AOCs on titanium foil using X-ray diffraction and X-ray photoelectron spectroscopy.

As has already been noted above, only qualitative models for the formation of such microstructures have been proposed to date. For example, some authors [14] discuss reasons for the formation of anatase microcones during the anodising of compact titanium in aqueous solutions of acids with fluorine ions. They suggest, in accordance with [21–23], that the mechanism of growth of anatase microcrystallites can be explained by the development of nanosized crystalline nuclei that form in defective sites on the metal/oxide interface under the influence of high local current density. However, they do not describe the effect of fluorine ions. It is believed [22, 23] that the growth of the crystalline component is due, firstly, to local heating, secondly, to compressive stresses that are present on the metal/oxide interface. It was also indicated that one of the reasons for the flower-like shape of the anatase microcones may be due to the reaction of oxygen evolution [38, 39]. When explaining the formation of MCCs by anodising titanium foil in a 1 M H_2SO_4 + 0.1 vol.% HF electrolyte, authors [18] presented a model whose determining factor was considered to be the existence of internal compressive stresses leading to the detachment of the oxide film and the appearance of hollow microcone formations. However, the authors did not give any reliable justification for the model.

Taking into account the available information on the growth of anatase microcone formations during anodising of compact titanium [14, 18, 21, 23], it can be assumed that the formation of hierarchical α-TiO_2 micro-nanostructures

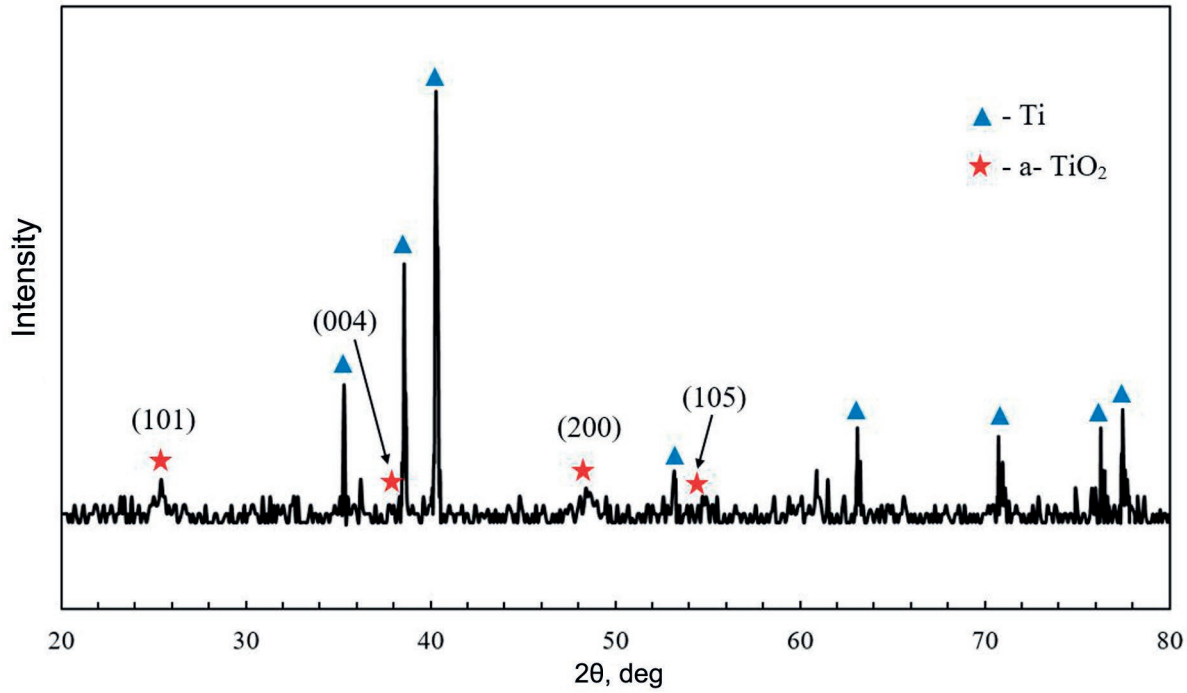

Fig. 8. X-ray diffraction (XRD) pattern of the sample of porous powder material made from titanium sponge after anodising in a 1M H_2SO_4 + 0.15 wt % HF electrolyte at j_m = 1,890 mA/g, t_a = 90 min

on the surface of TS PPM is also influenced by the heterogeneous relief of the surface of titanium sponge and oxygen-containing inclusions. Moreover, their effect on the process of crystallisations should increase with an increase in the current density of the galvanostatic process, which correlates well with the results of the study of the atomic structure and morphology.

Thus, the study of the growth, morphology, and atomic structure revealed that the proposed treatment conditions for porous materials from sintered powders of Ti sponge allow forming hierarchical micronastructured anodic oxide coatings characterised by a nanoporous amorphous matrix containing nanostructured anatase microcones.

4. Conclusions

The study of the influence of the conditions of the galvanostatic process on the growth of anodic oxide coatings on the samples of porous powder materials made from titanium sponge in a 1 M H_2SO_4 + 0.15 wt% HF electrolyte showed that anodising at a current density of $j_m \approx 202$ mA/g leads to the formation of an X-ray amorphous layer of TiO_2 with a thickness of about 250–350 nm and evenly distributed pores/tubes with effective diameters of (50±20) nm. Anodising at large current values of j_m in the range from 230 to 1,890 mA/g leads to the appearance of nanostructured α-TiO_2 microcones with base diameters and heights of up to 4–4.5 μm. These microcones are unevenly distributed in the X-ray amorphous oxide matrix. The obtained coatings on the surface of porous materials made from sintered powders of titanium sponge with a high specific area and a hierarchical micro/nanostructure are promising for a whole range of applications, in particular, for the design of devices for photocatalytic environment purification and production of superhydrophobic surfaces, which can be an area for further research.

Author contributions

N. M. Yakovleva: scientific supervision of research, concept of research, text writing, final conclusions. A. M. Shulga, K. V. Stepanova, A. N. Kokatev: studying the kinetics of growth and morphology by atomic force microscopy, generalising results, V. Lukianchuk: studying the morphology, elemental composition, atomic structure, scientific editing of the text, E. S. Chubieva: processing microscopic images, preparing figures.

Conflict of interests

The authors declare that they have no known competing financial interests or personal relationships that could have influenced the work reported in this paper.

References

1. Riboni F., Nguyen N. T., So S., Schmuki P. Aligned metal oxide nanotube arrays: key-aspects of anodic TiO_2 nanotube formation and properties. *Nanoscale Horizons*. 2016;1: 445–466. https://doi.org/10.1039/C6NH00054A

2. Yakovleva N. M., Kokatev A. N., Chupakhina E. A., Stepanova K. V., Yakovlev A. N., Vasil'ev S.G., Shul'ga A. M. Surface nanostructuring of metals and alloys. Part 2. Nanostructured anodic oxide films on Ti and Ti alloys. *Condensed Matter and Interphases*. 2016;18(1): 6–27. (In Russ., abstract in Eng.). Available at: https://elibrary.ru/item.asp?id=25946608

3. Lee K., Mazare A., Schmuki P. One-dimensional titanium dioxide nanomaterials: nanotubes. *Chemical Reviews*. 2014;114(1): 9385–9454. https://doi.org/10.1021/cr500061m

4. Macak J. M., Tsuchiya H., Ghicov A., Yasuda K., Hahn R., Bauer S., Schmuki P. TiO_2 nanotubes: selforganized electrochemical formation, properties and applications. *Current Opinion in Solid State and Materials Science*. 2007;11: 3–18. https://doi.org/10.1016/j.cossms.2007.08.004

5. Kulkarni M., Mazare A., Gongadze E., Perutkova Š., Kralj-Iglic V., Milošev I., Schmuki P., Iglic A., Mozetic M. Titanium nanostructures for biomedical applications. *Nanotechnology*. 2015;26: 1–18. https://doi.org/10.1088/0957-4484/26/6/062002

6. Kowalski D., Kim D., Schmuki P. TiO_2 nanotubes, nanochannels and mesosponge: Self-organized formation and applications. *Nano Today*. 2013;8(3): 235—264 https://doi.org/10.1016/j.nantod.2013.04.010

7. Kokatev A. N., Stepanova K. V., Yakovleva N. M., Tolstik V. E., Shelukhina A. I., Shulga A. M. Self-organization of a bioactive nanostructured oxide layer at the surface of sintered titanium sponge powder subjected to electrochemical anodization. *Technical Physics*. 2018;63(9): 1334–1340. https://doi.org/10.1134/S1063784218090062

8. Yoriya S., Mor G. K., Sharma S., Grimes C. A. Synthesis of ordered arrays of discrete, partially crystalline titania nanotubes by Ti anodization using diethylene glycol electrolytes. *Journal of Materials Chemistry*. 2008;18(28): 3332–3336. https://doi.org/10.1039/B802463D

9. Xiao X. F., Ouyang K. G., Liu R. F, Liang J. H. Anatase type titania nanotube arrays direct fabricated by anodization without annealing. *Applied Surface Science*. 2008;255(6): 3659–3663. https://doi.org/10.1016/j.apsusc.2008.10.014

10. Allam N. K., Grimes C. A. Room temperature one-step polyol synthesis of anatase TiO_2 nanotube arrays: photoelectrochemical properties. *Langmuir*. 2009;25(13): 7234–7240. https://doi.org/10.1021/la9012747

11. Liao Y., Wang X., Ma Y., Li J., Wen T., Jia L., Zhong Z., Wang L., Zhang D. New mechanistic insight of low temperature crystallization of anodic TiO_2 nanotube array in water. *Crystal Growth & Design*. 2016;16(4): 1786–1791. https://doi.org/10.1021/acs.cgd.5b01234

12. Lamberti A., Chiodoni A., Shahzad N., Bianco S., Quaglio M., Pirri C. F. Ultrafast room-temperature crystallization of TiO_2 nanotubes exploiting water-vapor treatment. *Scientific Reports*. 2015;5(1): 7808–7013. https://doi.org/10.1038/srep07808

13. Wang X., Zhang D., Xiang Q., Zhong Z., Liao Y. Review of water-assisted crystallization for TiO_2 nanotubes. *Nano-Micro Letters*. 2018;10(4): 77–105. https://doi.org/10.1007/s40820-018-0230-4

14. Wang C., Wang M., Xie K., Wu Q., Sun L., Lin Z., Lin C. Room temperature one-step synthesis of microarrays of N-doped flower-like anatase TiO_2 composed of well-defined multilayer nanoflakes by Ti anodization. *Nanotechnology*. 2011;22(30): 305607. https://doi.org/10.1088/0957-4484/22/30/305607

15. Huang J., Lai Y., Wang L., Li S., Ge M., Zhang K., Fuchs H., Chi L. Controllable wettability and adhesion on bioinspired multifunctional TiO_2 nanostructure surfaces for liquid manipulation. *Journal of Materials Chemistry A*. 2014;2(43): 8531–18538. https://doi.org/10.1039/C4TA04090B

16. Li S., Li Y., Wang J., Nan Y., Ma B., Liu Z., Gu J. Fabrication of pinecone-like structure superhydrophobic surface on titanium substrate and its self-cleaning property. *Chemical Engineering Journal*. 2016;290: 82–90. https://doi.org/10.1016/j.cej.2016.01.014

17. Rhee O., Lee G., Choi J. Highly ordered TiO_2 microcones with high rate performance for enhanced lithium-ion storage. *ACS Applied Materials & Interfaces*. 2016;8(23): 14558–14563. https://doi.org/10.1021/acsami.6b03099

18. Park J., Lee G., Choi J. Key anodization factors for determining the formation of TiO_2 microcones vs nanotubes. *Journal of The Electrochemical Society*. 2017;164(9): D640–D644. https://doi.org/10.1149/2.1601709jes

19. Park J., Choi J. Formation of well dispersed TiO_2 microcones; the 20% surface occupation. *Applied Surface Science*. 2018;448: 212–218. https://doi.org/10.1016/j.apsusc.2018.04.033

20. Park J., Kim S., Lee G., Choi J. RGO-coated TiO_2 microcones for high-rate lithium-ion batteries. *ACS*

Omega. 2018;3(8): 10205–10210. https://doi.org/10.1021/acsomega.8b00926

21. Xing J., Xia Z., Hu J., Zhang Y., Zhong L. Time dependence of growth and crystallization of anodic titanium oxide films in potentiostatic mode. *Corrosion Science*. 2013;75: 212–219. https://doi.org/10.1016/j.corsci.2013.06.004

22. Xing J., Li H., Xia Z., Hu J., Zhang Y., Zhong L. Formation and crystallization of anodic oxide films on sputter-deposited titanium in potentiostatic and potential-sweep modes. *Journal of The Electrochemical Society*. 2013;160(10): C503–C510. https://doi.org/10.1149/2.066310jes

23. Xing, J.-H. Xia Z.-B., Hu J.-F., Zhang Y.-H., Zhong L. Growth and crystallization of titanium oxide films at different anodization modes. *Journal of The Electrochemical Society*. 2013;160(6): 239–246. https://doi.org/10.1149/2.070306jes

24. Palma D. P. da S., Nakazato R. Z., Codaro E. N., Acciari H. A. Morphological and structural variations in anodic films grown on polished and electropolished titanium substrates. *Materials Research*. 2019;22: 1–98. https://doi.org/10.1590/1980-5373-MR-2019-0362

25. Zhang L., Duan Y., Gao R., Yang J., Wei K., Tang D., Fu T. The effect of potential on surface characteristic and corrosion resistance of anodic oxide film formed on commercial pure titanium at the potentiodynamic-aging mode. *Materials*. 2019;12(3): 370. https://doi.org/10.3390/ma12030370

26. Yoo H., Lee G., Choi J. Binder-free SnO_2–TiO_2 composite anode with high durability for lithium-ion batteries. *RSC Advances*. 2019;9: 6589–6595. https://doi.org/10.1039/C8RA10358E

27. Kim Y.-T., Youk J. H., Choi J. Inverse-direction growth of TiO_2 microcones by subsequent anodization in $HClO_4$ for increased performance of lithium-ion batteries. *ChemElectroChem*. 2020;7(5): 1057–1285. https://doi.org/10.1002/celc.202000114

28. Savich V. V, Bobrovskaya A. I., Taraikovich A. M., Bedenko S. A. Micro- and nanostructures surface foam particles of titanium powder and its influence on properties of porous materials from them. *Nanotechnologies of functional materials (NFM – 2012): proceeding of the international scientific and technical conference*, 27*–29 June 2012*. St. Petersburg: Polytechnic University Publ.; 2012. p. 523–529. (in Russ., abstract in Eng.)

29. Savich V. V. Metods of porous structure regulation of sintered materials from spongy powders of titanium. *Poroshkovaya metallurgiya*. 2016; 70–76. (in Russ., abstract in Eng.). Available at: https://elibrary.ru/item.asp?id=37590838

30. Shelukhina A. I., Stepanova K. V., Kokatev A. N., Tolstik V. E. Surface modification of porous materials made of sponge titanium powder by means of anodic oxidation. *Poroshkovaya metallurgiya*. 2015;38: 180–184. (in Russ., abstract in Eng.)

31. Yakovleva N. M., Shul'ga A. M., Lukiyanchuk I. V., Stepanova K. V., Kokatev A. N. Growth and crystallization of anodic oxide films on sintered titanium powders. In: *Powder metallurgy: Surface Engineering, New Powder Composite materials. Welding. Proc. 12th Int. Sym.., 7–9 April 2021, Minsk. In 2 p. Part 2*. Minsk: Belaruskaya nauka Publ.; 2021. p. 421–429. (in Russ., abstract in Eng.)

32. Yakovleva N. M., Shulga A. M., Stepanova K. V., Kokatev A. N., Rudnev V. S., Lukiyanchuk I. V., Kuryavyi V. G. Microcone anodic oxide films on sintered niobium powders. *Condensed Matter and Interphases*. 2020;22(1): 124–134. https://doi.org/10.17308/kcmf.2020.22/2536

33. Stepanova K. V., Yakovleva N. M., Kokatev A. N., Pettersson Kh. Nanoporous anodic oxide films on Ti–Al powder alloy. *Proceedings of Petrozavodsk State University. Natural and Engineering Sciences*. 2015;147(2): 81–86. (in Russ., abstract in Eng.). Available at: https://elibrary.ru/item.asp?id=23306599

34. Habazaki H., Uozumi M., Konno H., Shimizu K., Skeldon P., Thompson G. E. Crystallization of anodic titania on titanium and its alloys. *Corrosion Science*. 2003;45: 2063–2073. https://doi.org/10.1016/S0010-938X(03)00040-4

35. Habazaki H., Uozumi H., Konno H., Shimizu K., Skeldon P., Thompson G. E., Wood G. C. Breakdown of anodic films on titanium and its suppression by alloying. *Journal of Corrosion Science and Engineering*. 2003;6: 107. Available at: https://www.jcse.org/viewPaper/ID/206/fajeUDexa2dF4qbiJP7Hh6yvJ8mTNE

36. Nagesh Ch. R. V. S., Ramachandran C. S., Subramanyam R. B. Methods of titanium sponge production. *Transactions of the Indian Institute of Metals*. 2008;61(5): 341–348. https://doi.org/10.1007/s12666-008-0065-7

37. Beranek R., Hildebrand H., Schmuki P. Self-organized porous titanium oxide prepared in H_2SO_4/HF electrolytes. *Electrochemical and Solid-State Letters*. 2003;6(3): 12–14. https://doi.org/10.1149/1.1545192

38. Mazzarolo A., Curioni M., Vicenzo A., Skeldon P., Thompson G. E. Anodic growth of titanium oxide: Electrochemical behaviour and morphological evolution. *Electrochimica Acta*. 2012;75: 288–295. https://doi.org/10.1016/j.electacta.2012.04.114

39. Liu Z. J., Zhong X., Walton J., Thompson G. E. Anodic film growth of titanium oxide using the 3-electrode electrochemical technique: effects of oxygen evolution and morphological characterizations. *Journal of The Electrochemical Society*. 2016;163 (3): E75–E82. https://doi.org/10.1149/2.0181603jes

Information about the authors

Natalia M. Yakovleva, Dr. Sci. (Phys.–Math.), Full Professor, Professor at the Department of Information – Measuring Systems and Physical Electronics, Petrozavodsk State University (Petrozavodsk, Republic of Karelia, Russian Federation).

https://orcid.org/0000-0003-4294-0183
nmyakov@petrsu.ru, nmyakov@gmail.com

Alisa M. Shul'ga, Engineer, Petrozavodsk State University (Petrozavodsk, Republic of Karelia, Russian Federation).

https://orcid.org/0000-0002-3844-7110
shulga.alisa@gmail.com

Irina V. Lukiyanchuk, Cand. Sci. (Chem.), Senior Researcher, Institute of Chemistry, Far-Eastern Branch, Russian Academy of Sciences V(ladivostok, Russian Federation).

https://orcid.org/0000-0003-1680-4882
lukiyanchuk@ich.dvo.ru

Kristina V. Stepanova, Cand. Sci. (Tech.), Associate Professor, Petrozavodsk State University, (Petrozavodsk, Republic of Karelia, Russian Federation).

https://orcid.org/0000-0002-4737-497X
lady.cristin4ik@yandex.ru

Alexander N. Kokatev, Cand. Sci. (Tech.), Engineer, Petrozavodsk State University (Petrozavodsk, Republic of Karelia, Russian Federation).

https://orcid.org/0000-0002-9449-1482
nelan-oksid@bk.ru

Elena S. Chubieva, Engineer, Petrozavodsk State University (Petrozavodsk, Republic of Karelia, Russian Federation).

https://orcid.org/0000-0001-6782-8089
echubieva07@mail.ru

Received 23.06.2022; approved after reviewing 20.10.2022; accepted for publication 15.11.2022; published online 25.12.2022.

Translated by Irina Charychanskaya
Edited and proofread by Simon Cox